



# Chlorine initiated photooxidation of $(\text{CH}_3)_3\text{CC}(\text{O})\text{H}$ in the presence of $\text{NO}_2$ and photolysis at 254 nm. Synthesis and thermal stability of $(\text{CH}_3)_3\text{CC}(\text{O})\text{OONO}_2$



Diana Henao, Gustavo A. Argüello, Fabio E. Malanca\*

Instituto de Investigaciones en Fisicoquímica de Córdoba (INFIQC) CONICET – Departamento de Fisicoquímica, Facultad de Ciencias Químicas (Universidad Nacional de Córdoba), Ciudad Universitaria, X5000HUA Córdoba, Argentina

## ARTICLE INFO

### Article history:

Received 4 September 2014  
Received in revised form 30 October 2014  
Accepted 9 November 2014  
Available online 13 November 2014

### Keywords:

Peroxyacyl nitrates  
Photooxidation  
Atmospheric degradation  
Photochemistry

## ABSTRACT

Photooxidation of  $(\text{CH}_3)_3\text{CCHO}$  in the presence of  $\text{NO}_2$  leads to the formation of  $\text{CO}$ ,  $\text{CO}_2$ ,  $(\text{CH}_3)_3\text{CC}(\text{O})\text{OONO}_2$  (DMPPN), and  $(\text{CH}_3)_3\text{CCONO}_2$ . The synthesis of DMPPN and thermal decomposition studies were carried out. Pressure dependence was studied at 293 K from 6.0 to 1000 mbar. Kinetic parameters for DMPPN were determined between 293 and 308 K, at total pressures of 9.0 and 1000 mbar. The values found for the activation energy and pre-exponential factor were  $(109 \pm 3) \text{ kJ/mol}$ ,  $1.7 \times 10^{15} \text{ s}^{-1}$ , and  $(117 \pm 3) \text{ kJ/mol}$ ,  $5.2 \times 10^{16} \text{ s}^{-1}$  at these pressures, respectively. Thermal stability for DMPPN is similar to peroxyacyl nitrates already identified in the atmosphere, such as peroxyacetyl and peroxypropionyl nitrates. The quantum yield for photolysis at 254 nm of  $(\text{CH}_3)_3\text{CCHO}$  was determined to be  $0.60 \pm 0.05$ .

© 2014 Published by Elsevier B.V.

## 1. Introduction

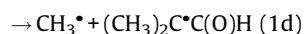
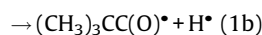
Aldehydes are important trace constituents of the atmosphere. They have natural and anthropogenic sources, with primary sources that are associated with vehicle exhaust, industrial activity, and secondary sources that are associated with the oxidation of volatile organic precursors [1]. Chemical removal of aldehydes from the troposphere can occur by gas phase reaction with OH and  $\text{NO}_3$  radicals, Cl atoms or by photolysis.

A major loss process of aldehydes is the abstraction of the aldehydic H atom, leading to carbonyl radicals  $\text{RC}(\text{O})^\bullet$  [1] which, in turn can be combined with  $\text{O}_2$ , to form the corresponding peroxyacyl radicals  $\text{RC}(\text{O})\text{OO}^\bullet$ . In polluted atmospheres, they could form stable peroxy acyl nitrates,  $\text{RC}(\text{O})\text{OONO}_2$ , which could add to the pool of phytotoxic, mutagenic, and irritant compounds forming the photochemical smog [2]. In laboratory studies, Cl atoms or  $\text{HO}^\bullet$  radicals are often used to generate peroxy radicals. Traditional  $\text{HO}^\bullet$  radical sources, such as  $\text{H}_2\text{O}_2$  or  $\text{HNO}_3$  photolysis using UV radiation ( $\lambda < 300 \text{ nm}$ ) [3,4] can complicate the kinetic analysis. Chlorine atoms are produced readily by the photolysis of  $\text{Cl}_2$  using black lamps ( $\lambda > 330 \text{ nm}$ ), where aldehyde photolysis is not a significant problem [1].

Trimethyl acetaldehyde (2,2 dimethyl propionyl aldehyde,  $(\text{CH}_3)_3\text{CCHO}$ , TMA) was studied by Le Crâne et al. [1], who

measured the rate constant with chlorine atoms and identified the peroxyacetyl nitrate that was formed,  $(\text{CH}_3)_3\text{CC}(\text{O})\text{OONO}_2$ , (2,2 dimethyl propionyl peroxyacetyl nitrate, DMPPN) in the presence of  $\text{O}_2$  and  $\text{NO}_2$ . In the present contribution, we went further in determining the kinetic parameters of the thermal decomposition of DMPPN as a function of pressure and temperature as well as its atmospheric thermal lifetime. This is relevant to evaluate its role as a reservoir species in the atmosphere [5,6] on account of the existence of similar peroxyacyl nitrates like peroxyacetyl (PAN), peroxypropionyl (PPN), and peroxybenzoyl (PBzN) nitrates [7,8].

On the other hand, photolysis is an important loss process that leads to the degradation of TMA in the atmosphere. There are several possible pathways for the photolytic rupture of TMA:



The quantum yield of TMA for the  $\text{HCO}^\bullet$  radical formation has been studied by Zhu et al. (1999) at wavelengths between 280 and 330 nm, obtaining values ranging from 0.18 to 0.92 [4]. This paper presents the new determination of the quantum yield at 254 nm.

\* Corresponding author. Tel.: +54 351 433 4169; fax: +54 351 433 4188.  
E-mail address: [fmalanca@fcq.unc.edu.ar](mailto:fmalanca@fcq.unc.edu.ar) (F.E. Malanca).

## 2. Materials and methods

### 2.1. Synthesis and characterization of DMPPN

The reagents were manipulated in a glass vacuum line equipped with two capacitance pressure gauges (0–760 Torr, MKS Baratron; 0–70 mbar, Bell and Howell). DMPPN was synthesized by the photolysis of mixtures containing  $(\text{CH}_3)_3\text{CCHO}$  (7.0 mbar),  $\text{Cl}_2$  (2.5 mbar),  $\text{NO}_2$  (3.0 mbar), and  $\text{O}_2$  (1000 mbar) at 295 K in a 5 L glass flask using black lamps ( $\lambda > 330$  nm) to initiate the oxidation of TMA using chlorine atoms. The progress of the synthesis was followed by infrared spectroscopy using a standard glass infrared gas cell (23.0 cm path length), located in the optical path of an IFS-28 FTIR spectrophotometer (resolution:  $2\text{ cm}^{-1}$ ) which allowed to monitor the temporal variation of reactants and products. The resulting mixture was collected by passing it through three traps at liquid–nitrogen temperature to remove oxygen excess. Subsequent distillation from 193 to 153 K allowed the elimination of excess of  $\text{ClNO}$ ,  $\text{HCl}$ , and carbon dioxide formed. The remaining mixture contained peroxyxynitrate, nitrate, and  $(\text{CH}_3)_3\text{CCHO}$ . Further distillation from 223 to 193 K removes TMA and nitrate. The batch containing the peroxyxynitrate had a residual of nitrate because of the similarity of the vapor pressure curves. The quantity of the impurity was less than 2% as measured by infrared spectroscopy using as reference the spectrum of the pure nitrate.

The gas phase infrared spectra of both species were recorded at room temperature in the range of  $4000\text{--}400\text{ cm}^{-1}$ , and the absorption cross-sections were calculated according to the following equation:

$$\sigma(\text{cm}^2\text{molecule}^{-1}) = \frac{\text{Abs} \times T(\text{K}) \times 31,79 \times 10^{-20}}{p(\text{mbar}) \times l(\text{cm})}$$

where  $T$  is the temperature,  $p$  is the pressure and  $l$  is the optical path. The pressures of DMPPN ranged from 1.0 to 6.0 mbar.

The infrared spectrum of DMPPN (main bands at 790, 1000, 1058, 1300, 1735, 1820  $\text{cm}^{-1}$ ) is in good agreement with all the bands reported by Jagiella et al., 2000 [9]. In addition, density functional theory has been used to evaluate the optimized geometries, vibrational frequencies, and intensities using the Gaussian09 software package [10] in conjunction with GaussView 5.0 [11]. The hybrid density functional B3LYP with the 6-31++G(d,p) basis set was used in all calculations.

Thermal stability was determined by the addition of  $\text{NO}$  in the temperature range between 293 and 308 K, at 9.0 and 1000 mbar total pressure. At 293 K, the pressure dependence of the rate constant was measured between 6.0 and 1000 mbar total pressure, reached by adding the necessary amount of He. The temporal variation of the infrared band at  $1734\text{ cm}^{-1}$  corresponding to the peroxyxynitrate was used to determine the rate constant.

The photooxidation mechanism of TMA in the presence of  $\text{NO}_2$  was corroborated by comparing the experimental temporal evolution of reactants and products with a kinetic model (KINTECUS) [12].

### 2.2. Photolysis and quantum yield of TMA at 254 nm

In order to determine the quantum yield of TMA, we previously measured its UV absorption cross sections ( $\sigma$ ) using a standard UV gas cell (optical path 10 cm) located on the optical axis of a UV–vis spectrophotometer with a diode array detector. A calibration curve was obtained for pressures ranging between 5.0 and 20.0 mbar.

Photolysis experiments were performed using a quartz cell with an optical path of 23 cm and a low-pressure mercury lamp (15 W). TMA was irradiated alone and in the presence of cyclohexane (90 mbar) to trap the radicals formed so as to ensure that they did

not contribute to secondary reactions. Control experiments were performed to check whether the aldehyde concentration changed as a consequence of dark or heterogeneous reactions without detecting any appreciable loss. The course of the reaction was followed at  $1750\text{ cm}^{-1}$  because no reaction products absorb this frequency.

### 2.3. Reagents

Commercially available samples of trimethyl acetaldehyde, cyclohexane (Sigma–Aldrich),  $\text{CF}_3\text{COCl}$  (PCR Research Chemicals Inc.),  $\text{O}_2$  (AGA), He (AGA) were used.  $\text{Cl}_2$  (>99%) was prepared by dehydration of  $\text{HCl}$  and  $\text{NO}_2$  (>99%) that was obtained from thermal decomposition of  $\text{Pb}(\text{NO}_3)_2$ .

## 3. Results and discussion

### 3.1. Photooxidation of TMA in the presence of $\text{NO}_2$

The spectra obtained in the photooxidation of  $(\text{CH}_3)_3\text{CCHO}$  before and 15 min after irradiation as well as their subtraction showing the resulting products are depicted in Fig. 1. The trace corresponding to the products (third trace from top to bottom) reveals at a glance the formation of  $\text{CO}_2$  (2346 and  $667\text{ cm}^{-1}$ ). Further inspection reveals characteristic peaks of a peroxyxynitrate (794,  $1735\text{ cm}^{-1}$ ) and those of a nitrate (862,  $1648\text{ cm}^{-1}$ ). Their identities ( $(\text{CH}_3)_3\text{CC}(\text{O})\text{OONO}_2$  and  $(\text{CH}_3)_3\text{CONO}_2$ , *t*-butyl nitrate) were positively addressed through their synthesis and successive distillations as described above as well as all the calculations carried out with the Gaussian Package. Furthermore, beyond the good agreement between our experimental and theoretical spectra, we had a remarkable coincidence with the spectrum published by Jagiella et al. [9].

Table 1 lists the infrared absorption cross-sections at the main peaks for DMPPN and its comparison with data for selected peroxy acyl nitrates: PAN ( $\text{CH}_3\text{C}(\text{O})\text{OONO}_2$ , peroxyacetyl nitrate), PPN ( $\text{CH}_3\text{CH}_2\text{C}(\text{O})\text{OONO}_2$ , peroxypropionyl nitrate), PnBN ( $\text{CH}_3(\text{CH}_2)_2\text{C}(\text{O})\text{OONO}_2$ , peroxy-*n*-butyryl nitrate) [8].

The integrated band areas ( $\text{cm molecule}^{-1}$ ) at 293 K of the principal absorption bands were determined as:  $1.68 \times 10^{-17}$  at  $790\text{ cm}^{-1}$  (integration range 818–773) and  $3.47 \times 10^{-17}$  at

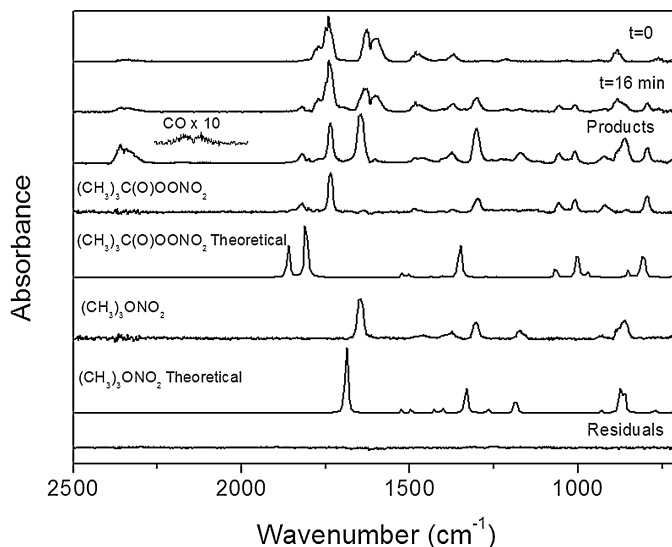


**Fig. 1.** Identification of products in the photooxidation of TMA in the presence of  $\text{NO}_2$ . From top to bottom: before photolysis; after 16 min irradiation; products;  $(\text{CH}_3)_3\text{CC}(\text{O})\text{OONO}_2$  (experimental and calculated),  $(\text{CH}_3)_3\text{CONO}_2$  (idem). The last trace corresponds to residuals (4 $\times$ ).

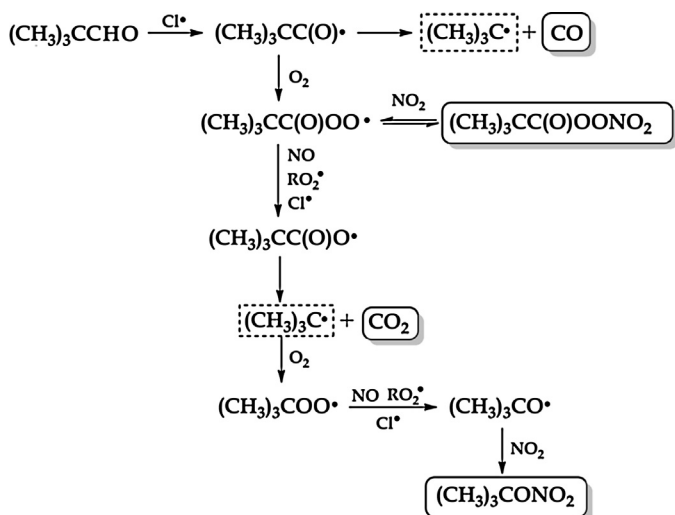
**Table 1**  
Infrared absorption cross-sections for DMPPN and comparison with selected peroxy nitrates.

Wavenumbers (cm <sup>-1</sup> )	$\sigma \times 10^{19}$ (cm <sup>2</sup> molecule <sup>-1</sup> )				Assignments
	PAN	PPN	PnBN	DMPPN	
790				9.44 (0.09)	$\delta(\text{NO}_2)$
794	9.5 (0.2)				
796		9.04 (0.09)	5.40 (0.09)		
1000				7.53 (0.08)	$\nu(\text{C}-\text{O})$
1037			2.59 (0.05)		
1044		2.70 (0.09)			
1163	12.1 (0.3)				
1735				23.8 (0.2)	$\nu_{\text{as}}(\text{NO}_2)$
1738		20.6 (0.2)			
1741	23.9 (0.6)		14.5 (0.2)		
1820				5.4 (0.5)	$\nu(\text{C}=\text{O})$
1834			6.63 (0.06)		
1835		5.97 (0.07)			
1842	7.4 (0.3)				

1735 cm<sup>-1</sup> (integration range 1765–1711) for DMPPN;  $1.43 \times 10^{-17}$  at 862 cm<sup>-1</sup> (integration range 879–836) and  $2.45 \times 10^{-17}$  at 1648 cm<sup>-1</sup> (integration range 1675–1615) for *t*-butyl nitrate. In particular, the last value agrees with the average for organic nitrates RONO<sub>2</sub> ( $2.5 \times 10^{-17}$  cm molecule<sup>-1</sup>) informed in literature [13,14].

Once identified and characterized by IR spectroscopy, both the peroxy nitrates and the nitrate, we proceeded to their quantification as well as the determination of the mechanism photo-oxidation of TMA.

The reaction mechanism postulated according to the products observed and the kinetic analysis performed is shown in Scheme 1. Reaction of chlorine atoms with (CH<sub>3</sub>)<sub>3</sub>CCO• initiates the photooxidation leading to the formation of (CH<sub>3</sub>)<sub>3</sub>CCO• radicals, as reported by other workers [1]. Acyl radicals could either decompose, leading to the formation of CO and (CH<sub>3</sub>)<sub>3</sub>C• radicals,



**Scheme 1.** Reaction mechanism of photooxidation of TMA in the presence of NO<sub>2</sub>.

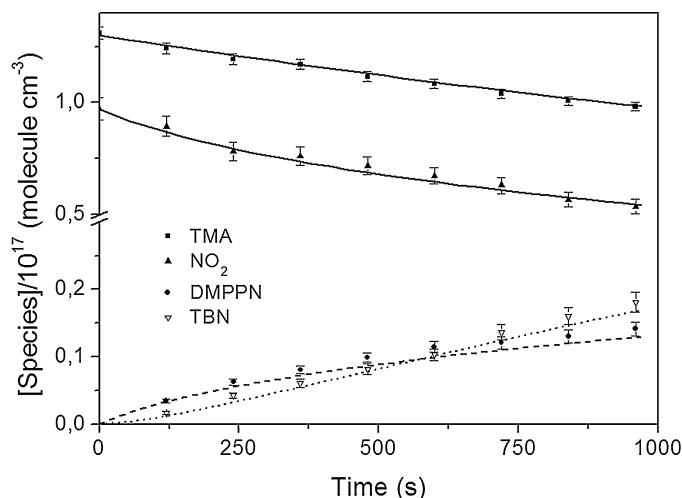


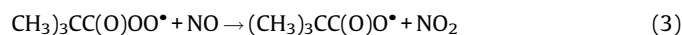
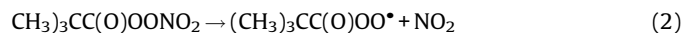
**Fig. 2.** Photooxidation of TMA in the presence of NO<sub>2</sub>. Temporal variation of reactants and products: experimental (symbols), calculated-KINTECUS Model (lines).

or react with O<sub>2</sub>, giving the peroxy radicals (CH<sub>3</sub>)<sub>3</sub>CC(O)OO•. The formation of DMPPN is consistent with a relatively high concentration of NO<sub>2</sub> while the formation of *t*-butyl nitrate is a consequence of both the loss of CO by the acyl radical following the absorption of the photon and the slow thermal decomposition of DMPPN.

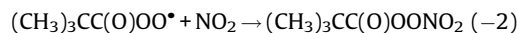
Temporal variations of reactants and main products are presented in Fig. 2 and the complete set of reactions used to model the system is shown in Table 2. The listed rate constant values were either taken from the literature, determined experimentally in this work, or assumed for similar reactions, when kinetic data were not available. As can be seen in Fig. 2, there is a good agreement between experimental and calculated (KINTECUS) data corroborating the proposed mechanism.

### 3.2. Thermal stability of DMPPN

The temperature dependence of the first-order rate constant was measured at 10.0 mbar and temperatures ranging from 293 to 308 K. The decomposition was carried out by adding an excess of NO in the system sufficient to titrate the peroxy radicals (Reaction (3)) formed by the thermal decomposition (Reaction (2)):



while avoiding the occurrence of reaction (-2)



Owing to Reaction (3), the concentration of NO<sub>2</sub> increases in the system and, consequently, so does the velocity of reaction (-2). Under these conditions, the rate constant for the disappearance of peroxy nitrates ( $k_{\text{obs}}$ ) does not quite reflect the value of  $k_2$  and, therefore, it must be corrected by multiplying the factor  $\{1 + k_{-2} [\text{NO}_2]/k_3 [\text{NO}]\}$ . This correction has been extensively used [26–31] and, in our system, led to a correction of less than 3% in  $k_{\text{obs}}$ .

First-order decay plots following the disappearance of DMPPN at 1735 cm<sup>-1</sup> were obtained at different temperatures and pressures. After linear fitting, rate constants were obtained. Fig. 3 shows the pressure dependence of  $k_2$  between 6.0 and 1000 mbar at 293 K. There is no significant dependence of the rate constant beyond 500 mbar. Nevertheless, our experimental

**Table 2**

Set of reactions used to fit the concentration profiles.

Rate constant values ( <i>k</i> )	Reaction	Comments/Refs.
$3.7 \times 10^{-4}$	$\text{Cl}_2 + h\nu \rightarrow 2\text{Cl}$	Derived from experimental data
$4.0 \times 10^{-4}$	$\text{NO}_2 + h\nu \rightarrow \text{NO} + \text{O}$	Derived from experimental data
$1.0 \times 10^{-11}$	$\text{O} + \text{NO}_2 \rightarrow \text{NO} + \text{O}_2$	[15]
$1.1 \times 10^{-12}$	$\text{O} + \text{NO} \rightarrow \text{NO}_2$	[23]
$1.2 \times 10^{-10}$	$(\text{CH}_3)_3\text{CCHO} + \text{Cl} \rightarrow (\text{CH}_3)_3\text{CC}(\text{O})^* + \text{HCl}$	Varied from $(0.9 - 1.5) \times 10^{-10}$ [1]
$1.2 \times 10^{-12}$	$(\text{CH}_3)_3\text{CCHO} + \text{O} \rightarrow (\text{CH}_3)_3\text{CC}(\text{O})^* + \text{OH}$	Similar to $(\text{CH}_3)_2\text{CHC}(\text{O})\text{H} + \text{O}$ [18,19]
$2.7 \times 10^{-11}$	$(\text{CH}_3)_3\text{CCHO} + \text{OH} \rightarrow (\text{CH}_3)_3\text{CC}(\text{O})^* + \text{H}_2\text{O}$	[21]
$3.2 \times 10^{-12}$	$(\text{CH}_3)_3\text{CC}(\text{O})^* + \text{O}_2 \rightarrow (\text{CH}_3)_3\text{CC}(\text{O})\text{OO}^*$	[9]
$4.3 \times 10^5$	$(\text{CH}_3)_3\text{CC}(\text{O})^* \rightarrow (\text{CH}_3)_3\text{C}^* + \text{CO}$	Varied from $(2.5 - 4.5) \times 10^5$ [16]
$2.8 \times 10^{-12}$	$(\text{CH}_3)_3\text{CC}(\text{O})\text{OO}^* + \text{NO}_2 \rightarrow (\text{CH}_3)_3\text{CC}(\text{O})\text{OONO}_2$	Similar to $\text{CH}_3\text{C}(\text{O})\text{OO} + \text{NO}_2$ [17]
$1.5 \times 10^{-4}$	$(\text{CH}_3)_3\text{CC}(\text{O})\text{OONO}_2 \rightarrow (\text{CH}_3)_3\text{CC}(\text{O})\text{OO}^* + \text{NO}_2$	This work
$7.7 \times 10^{-11}$	$(\text{CH}_3)_3\text{CC}(\text{O})\text{OO}^* + \text{Cl}^* \rightarrow (\text{CH}_3)_3\text{CC}(\text{O})\text{O}^* + \text{ClO}^*$	Similar to $\text{CH}_3\text{OO} + \text{Cl}$ [23]
$3.0 \times 10^{-11}$	$(\text{CH}_3)_3\text{CC}(\text{O})\text{OO}^* + \text{NO} \rightarrow (\text{CH}_3)_3\text{CC}(\text{O})\text{O}^* + \text{NO}_2$	[15]
$1.45 \times 10^{-11}$	$2 (\text{CH}_3)_3\text{CC}(\text{O})\text{OO}^* \rightarrow 2 (\text{CH}_3)_3\text{CC}(\text{O})\text{O}^* + \text{O}_2$	[1]
$1.0 \times 10^9$	$(\text{CH}_3)_3\text{CC}(\text{O})\text{O}^* \rightarrow (\text{CH}_3)_3\text{C}^* + \text{CO}_2$	Fast thermal decomposition [1]
$3.5 \times 10^{-12}$	$(\text{CH}_3)_3\text{C}^* + \text{O}_2 \rightarrow (\text{CH}_3)_3\text{COO}^*$	[16]
$7.7 \times 10^{-11}$	$(\text{CH}_3)_3\text{COO}^* + \text{Cl} \rightarrow (\text{CH}_3)_3\text{CO}^* + \text{ClO}^*$	[23]
$4.3 \times 10^{-12}$	$(\text{CH}_3)_3\text{COO}^* + \text{NO} \rightarrow (\text{CH}_3)_3\text{CO}^* + \text{NO}_2$	[24]
$2.09 \times 10^{-13}$	$(\text{CH}_3)_3\text{COO}^* + \text{NO} \rightarrow (\text{CH}_3)_3\text{CONO}_2$	[25]
$1.43 \times 10^{-11}$	$2 (\text{CH}_3)_3\text{COO}^* \rightarrow 2 (\text{CH}_3)_3\text{CO}^* + \text{O}_2$	Varied from $1$ to $2 \times 10^{-11}$ [1,2]
$2.5 \times 10^{-11}$	$(\text{CH}_3)_3\text{CO}^* + \text{NO} \rightarrow (\text{CH}_3)_3\text{CONO}$	[20]
$3.50 \times 10^{-11}$	$(\text{CH}_3)_3\text{CO}^* + \text{NO}_2 \rightarrow (\text{CH}_3)_3\text{CONO}_2$	[22]
$1.25 \times 10^{-11}$	$(\text{CH}_3)_3\text{CC}(\text{O})\text{OO}^* + (\text{CH}_3)_3\text{COO}^* \rightarrow (\text{CH}_3)_3\text{CC}(\text{O})\text{O}^* + (\text{CH}_3)_3\text{CO}^* + \text{O}_2$	[2]
$1.4 \times 10^3$	$(\text{CH}_3)_3\text{CO}^* \rightarrow \text{CH}_3\text{C}(\text{O})\text{CH}_3 + \text{CH}_3^*$	Varied from 800 to 2000 [1,20,9,22]

Units: Unimolecular reaction ( $\text{s}^{-1}$ ). Bimolecular reactions ( $\text{cm}^3 \text{molecule}^{-1} \text{s}^{-1}$ ).

runs – used to derive the activation energy at high pressures – were conducted at a total pressure of 1000 mbar, ensuring that the kinetic studies were performed under the high-pressure regime. The activation energy ( $E_a$ ) and pre-exponential factor obtained at 9.0 and 1000 mbar were  $E_a = (109 \pm 3) \text{ kJ/mol}$ ,  $A = 1.7 \times 10^{15}$ ; and  $E_a = (117 \pm 3) \text{ kJ/mol}$ ,  $A = 5.2 \times 10^{16}$ , respectively. As can be seen,  $E_a$  decreases with the decrease in total pressure, in agreement with unimolecular reaction rate theories.

The kinetic parameters obtained at 1 bar are similar to those available in the bibliography for the most abundant peroxy nitrates detected in the atmosphere, PAN and PPN ( $E_a = 113 \text{ kJ/mol}$ ,  $A = 2.5 \times 10^{16}$ ;  $E_a = 116 \text{ kJ/mol}$ ,  $A = 7.2 \times 10^{16}$  respectively) [32] and, therefore, all of them show similar thermal stabilities. Due to the atmospheric thermal profile, the thermal lifetime for DMPPN varies as a function of altitude. It equals approximately

2 days at 2 km, rising steeply to 30 days at 4 km, increasing rapidly to reach decades at altitudes higher than 6 km. The lifetime is greater than that of PAN, suggesting that, if DMPPN is formed in the atmosphere, it should act as reservoir species.

### 3.3. Photolysis and quantum yield at 254 nm

TMA was photolyzed alone and in the presence of cyclohexane at 254 nm to have an estimation of the quantum yield. In the former case, the decay of TMA observed is higher, corroborating that the *c*-hexane added acts effectively as a radical scavenger of radicals formed by the photolytic rupture of the molecule protecting the TMA for further reactions. Because our goal was to measure just the primary process of the absorption of the photon, we performed all the subsequent experiments in the presence of a large excess of cyclo-hexane in order to trap any radical formed thus preventing the occurrence of radical–molecule reactions.

We irradiated gas mixtures using a low-pressure Hg lamp and derived the quantum yield from the following equation:

$$\frac{k_{(\text{CH}_3)_3\text{CCHO}}}{k_{\text{actinometer}}} = \frac{\sigma_{254\text{nm}}(\text{CH}_3)_3\text{CCHO} \times \phi_{254\text{nm}}(\text{CH}_3)_3\text{CCHO}}{\sigma_{254\text{nm}}\text{actinometer} \times \phi_{254\text{nm}}\text{actinometer}}$$

where  $k$ ,  $\sigma_{254\text{nm}}$  and  $\phi_{254\text{nm}}$  correspond to the rate constant for the disappearance, the absorption cross-sections and the quantum yield at 254 nm, respectively. Trifluoroacetyl chloride,  $\text{CF}_3\text{C}(\text{O})\text{Cl}$  ( $\sigma_{254\text{nm}} = 6.86 \times 10^{-20} \text{ cm}^2 \text{ molecule}^{-1}$ ,  $\phi \cong 1.0$ ) [33,34] was employed as actinometer. The absorption cross section of TMA at 254 nm (taken from the calibration curve) was  $(9.1 \pm 0.4) \times 10^{-21} \text{ cm}^2 \text{ molecule}^{-1}$ . The analysis of the spectra reveals the formation of carbon monoxide, isobutane ( $(\text{CH}_3)_3\text{CH}$ ) and formaldehyde as a consequence of three different processes, namely the scission of the C–C bond, the O–H bond and the extrusion of CO. The appearance of the products could be rationalized through the following reactions:

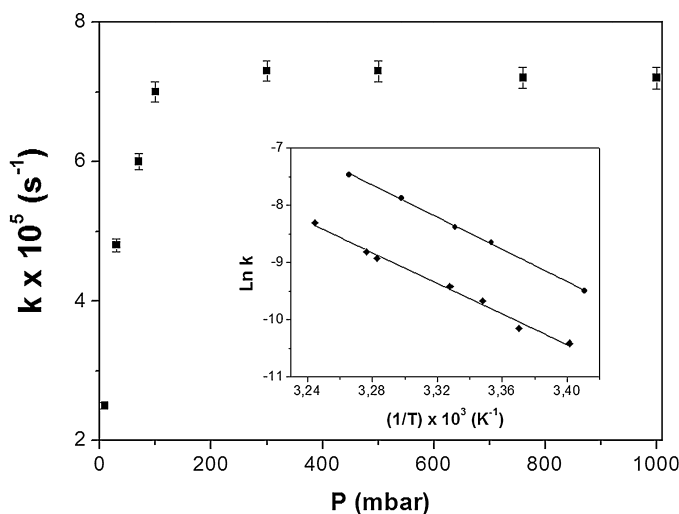
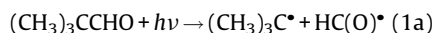
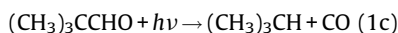
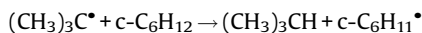
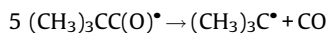
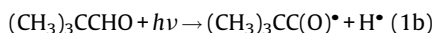
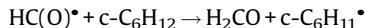
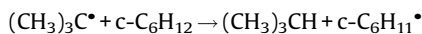


**Fig. 3.** Thermal decomposition of DMPPN as a function of total pressure at 293 K. Insert shows the results as a function of temperature at 9.0 (diamonds) and 1000 mbar (circles) total pressure.





Quantification of the disappearance of TMA leads a global value of  $0.60 \pm 0.05$  for the total quantum yield in good agreement with values derived for similar aldehydes by other workers, for example, 0.65 for propanal [35] and 0.63 for isobutanal [36]. On the other hand, the quantification of formaldehyde gives the primary quantum yield for the C–C scission ( $\varphi_a = 0.32$ ) while the quantification of carbon monoxide gives the sum of ( $\varphi_b + \varphi_c$ ) = 0.30.

These results agree with the values of quantum yield reported for similar aldehydes ( $\varphi_a$  and  $\varphi_b$ , respectively): 0.28 and 0.32 for  $\text{C}_2\text{H}_5\text{CHO}$ ; 0.20 and 0.40 for  $(\text{CH}_3)_2\text{CHCHO}$ .

## Acknowledgments

Financial support from CONICET, ANPCYT, and SECyT-UNC is gratefully acknowledged.

## References

- J.P. Le Crâne, E. Villenave, M.D. Hurley, T.J. Wallington, S. Nishida, K. Takahashi, Y. Matsumi, Atmospheric chemistry of pivalaldehyde and isobutiraldehyde: kinetics and mechanism of reactions with Cl atoms, fate of  $(\text{CH}_3)_3\text{CC(O)}$  and  $(\text{CH}_3)_2\text{CHC(O)}$  radicals, and self-reaction kinetics of  $(\text{CH}_3)_3\text{CC(O)}_2$  and  $(\text{CH}_3)_2\text{CHC(O)}_2$  radicals, *J. Phys. Chem. A* 108 (2004) 795–805.
- A. Tomas, R. Lesclaux, Self-reaction kinetics of the  $(\text{CH}_3)_2\text{CHC(O)}_2$  and  $(\text{CH}_3)_3\text{CC(O)}_2$  acylperoxy radicals between 275 and 363 K, *Chem. Phys. Lett.* 319 (2000) 521–528.
- R.D. Martinez, A.A. Buitrago, N.W. Howell, C.H. Hearn, A. Joens, The near U.V. absorption spectra of several aliphatic aldehydes and ketones at 300 K, *Atmos. Environ. Part A* 26 (1992) 785–792.
- L. Zhu, T. Cronin, A. Narang, Wavelength-dependent photolysis of *i*-pentanal and *t*-pentanal from 280 to 330 nm, *J. Phys. Chem. A* 103 (1999) 7248–7253.
- F. Kirchner, L.P. Thuener, I. Barnes, K.H. Becker, B. Donner, F. Zabel, Thermal lifetimes of peroxy nitrates occurring in the atmospheric degradation of oxygenated fuel additives, *Environ. Sci. Technol.* 31 (1997) 1801–1804.
- J.M. Roberts, The atmospheric chemistry of organic nitrates, *Atmos. Environ.* (1990) 243–287.
- J.S. Gaffney, N.A. Marley, M.M. Cunningham, P.V. Doskey, Measurements of peroxyacyl nitrates (PANS) in Mexico City: implications for megacity air quality impacts on regional scales, *Atmos. Environ.* 33 (1999) 5003–5012.
- S. Glavas, N. Moschonas, Determination of PAN, PPN, PnBN and selected pentyl nitrates in Athenes, Greece, *Atmos. Environ.* 35 (2001) 5467–5475.
- S. Jagiella, H.G. Libuda, F. Zabel, Thermal stability of carbonyl radicals. Part I. Straight-chain and branched  $\text{C}_4$  and  $\text{C}_5$  acyl radicals, *Phys. Chem. Chem. Phys.* 2 (2000) 1175–1181.
- M.J. Frisch, G.W. Trucks, H.B. Schlegel, G.E. Scuseria, A. Robb, J.R. Cheeseman, V. G. Zakrzewski, J.A. Montgomery Jr., R.E. Stratmann, J.C. Burant, S. Dapprich, J.M. Millam, A.D. Daniels, K.N. Kudin, M.C. Strain, O. Farkas, J. Tomasi, V. Barone, M. Cossi, R. Cammi, B. Mennucci, C. Pomelli, C. Adamo, S. Clifford, J. Ochterski, G.A. Petersson, P.Y. Ayala, Q. Cui, K. Morokuma, D.K. Malick, A.D. Rabuck, K. Raghavachari, J.B. Foresman, J. Cioslowski, J.V. Ortiz, A.G. Baboul, B.B. Stefanov, G. Liu, A. Liashenko, P. Piskorz, I. Komaromi, R. Gomperts, R.L. Martin, D.J. Fox, T. Keith, M.A. Al-Laham, C.Y. Peng, A. Nanayakkara, C. Gonzalez, M. Challacombe, P.M.W. Gill, B. Johnson, W. Chen, M.W. Wong, J.L. Andres, C. Gonzalez, M. Head-Gordon, E.S. Replogle, J.A. Pople, Gaussian 98, Revision A.7, Gaussian, Inc., Pittsburgh, PA, 1998.
- [11] GaussView, Version 5, Roy Dennington, Todd Keith and John Millam, Semichem Inc., Shawnee Mission KS, 2009.
- [12] Ianni J.C. K. INTECUS V 4.0.0.
- [13] E.C. Tuazon, S.M. Aschmann, R. Atkinson, Products of the gas-phase reaction of the oh radical with the dibasic Ester  $\text{CH}_3\text{OC(O)CH}_2\text{CH}_2\text{C(O)OCH}_3$ , *Environ. Sci. Technol.* 33 (1999) 2885–2890.
- [14] F. Cavalli, I. Barnes, K.H. Becker, FT-IR kinetic and product study of the OH radical and Cl-atom – initiated oxidation of dibasic esters, *Int. J. Chem. Kinet.* 33 (2001) 431–439.
- [15] R. Atkinson, D.L. Baulch, R.A. Cox, J.N. Crowley, R.F. Hampson, R.G. Hynes, M.E. Jenkin, M.J.J. Rossi Troe, Evaluated kinetic and photochemical data for atmospheric chemistry: volume I – gas phase reactions of Ox, HOx, NOx and SOx species, *Atmos. Chem. Phys.* 4 (2004) 1461–1738.
- [16] S. Dusanter, L. Elmaimouni, C. Fittschen, B. Lemoine, P. Devolder, Falloff curves for the unimolecular decomposition of two acyl radicals:  $\text{RCO} (+\text{M})$  ( $\text{R} + \text{CO} (+\text{M})$ ) by pulsed laser photolysis coupled to time-resolved infrared diode laser absorption, *Int. J. Chem. Phys.* 37 (2005) 611–624.
- [17] J. Sehested, L.K. Christensen, T. Molgelberg, O.J. Nielsen, T.J. Wallington, A. Guschin, J.J. Orlando, G.S. Tyndall, Absolute and relative rate constants for the reactions  $\text{CH}_3\text{C(O)O}_2 + \text{NO}$  and  $\text{CH}_3\text{C(O)O}_2 + \text{NO}_2$  and the thermal stability of  $\text{CH}_3\text{C(O)O}_2\text{NO}_2$ , *J. Phys. Chem. A* 102 (2004) 1779–1789.
- [18] D.L. Singleton, R.S. Irwin, R.J. Cvetanovic, Arrhenius parameters for the reaction of  $\text{O}(^3\text{P})$  atoms with several aldehydes and the trend in aldehydic CH bond dissociation energies, *Can. J. Chem.* 55 (1977) 3317–3321.
- [19] J.T. Herron, Evaluated chemical kinetic data for the reactions of atomic oxygen  $\text{O}(^3\text{P})$  with saturated organic compounds in the gas phase, *J. Phys. Chem. Ref. Data* 17 (1988) 967.
- [20] M. Blitz, M.J. Pilling, S.H. Robertson, P.W. Seakins, Direct studies on the decomposition of the tert-butoxy radical and its reaction with NO, *J. Phys. Chem. Chem. Phys.* 1 (1999) 73–80.
- [21] B. D'Anna, O. Andresen, Z. Gefen, C.J. Nielsen, Kinetic study of OH and  $\text{NO}_3$  radical reactions with 14 aliphatic aldehydes, *Phys. Chem. Chem. Phys.* 3 (2001) 3057–3063.
- [22] R. Atkinson, S. Roger, Atmospheric reactions of alkoxy and *b*-hydroxyalkoxy radicals, *Int. J. Chem. Kinet.* 29 (1997) 99–111.
- [23] W.B. DeMore, S.P. Sander, D.M. Golden, R.F. Hampson, M.J. Kurylo, C.J. Howard, A.R. Ravishankara, C.J. Kolb, M.J. Molina, Chemical Kinetic and Photochemical Data for Use in Stratospheric Modeling: Evaluation No. 11 of the NASA Panel for Data Evaluation, JPL Publication, 1994, pp. 26–94.
- [24] S. Langer, E. Ljungstrom, T. Ellermann, O.J. Nielsen, J. Sehested, Pulse radiolysis study of reactions of alkyl and alkylperoxy radicals originating from methyl tert-butyl ether in the gas phase, *Chem. Phys. Lett.* 240 (1995) 499–505.
- [25] R. Atkinson, S.M. Aschmann, A.M. Winer, Alkyl nitrate formation from the reaction of a series of branched  $\text{RO}_2$  radicals with NO as a function of temperature and pressure, *J. Atmos. Chem.* 5 (1987) 91–102.
- [26] A. Tomas, R. Lesclaux, Self-reaction kinetics of the  $(\text{CH}_3)_2\text{CHC(O)}_2$  and  $(\text{CH}_3)_3\text{C(O)}_2$  acylperoxy radicals between 275 and 363 K, *Chem. Phys. Lett.* 319 (2000) 521–528.
- [27] Christensen L.K. Wallington, T.J. Guschin, A. Hurlley, Atmospheric degradation mechanism of  $\text{CF}_3\text{OCH}_3$ , *J. Phys. Chem. A* 103 (1999) 4202–4208.
- [28] F. Zabel, F. Kirchner, K.H. Becker, Thermal decomposition of  $\text{CF}_3\text{C(O)O}_2\text{NO}_2$ ,  $\text{CCl}_2\text{FC(O)O}_2\text{NO}_2$ ,  $\text{CCl}_2\text{FC(O)O}_2\text{NO}_2$ , and  $\text{CCl}_3\text{C(O)O}_2\text{NO}_2$ , *Int. J. Chem. Kinet.* 26 (1994) 827–845.
- [29] J. Sehested, L.K. Christensen, O.J. Nielsen, M. Bilde, T.J. Wallington, W.F. Schneider, J.J. Orlando, G.S. Tyndall, Atmospheric chemistry of acetone: kinetic study of the  $\text{CH}_3\text{C(O)CH}_2\text{O}_2 + \text{NO}/\text{NO}_2$  reactions and decomposition of  $\text{CH}_3\text{C(O)CH}_2\text{O}_2\text{NO}_2$ , *Int. J. Chem. Kinet.* 30 (1998) 475–489.
- [30] D. Henao, F.E. Malanca, M.S. Chiappero, G.A. Argüello, Thermal stability of peroxy acyl nitrates formed in the oxidation of  $\text{C}_x\text{F}_{2x+1}\text{CH}_2\text{C(O)H}$  ( $x = 1,6$ ) in the presence of  $\text{NO}_2$ , *J. Phys. Chem. A* 117 (2013) 3625–3629.
- [31] A.G. Bossolasco, J.A. Vila, M.A. Burgos Paci, F.E. Malanca, G.A. Argüello, A new perfluorinated peroxy nitrate,  $\text{CF}_3\text{CF}_2\text{CF}_2\text{CF}_2\text{OONO}_2$ . Synthesis, characterization and atmospheric implications, *Chem. Phys.* 441 (2014) 11–16.
- [32] F. Kirchner, A. Mayer-Figge, F. Zabel, K.H. Becker, The thermal stability of peroxy nitrates, *Int. J. Chem. Kinet.* 31 (1999) 127–144.
- [33] R. Meller, G.K. Moortgat,  $\text{CF}_3\text{C(O)Cl}$ : temperature-dependent (223–298 K) absorption cross-sections and quantum yields at 254 nm, *J. Photochem. Photobiol. A Chem.* 108 (1997) 105–116.
- [34] D.E. Weibel, G.A. Argüello, E.R. De Staricco, E.H. Staricco, Quantum yield in the gas phase photolysis of perfluoroacetyl chloride: a comparison with related compounds, *J. Photochem. Photobiol. A: Chem.* 86 (1995) 27–31.
- [35] J.G. Calvert, A. Mellouki, J.J. Orlando, M.J. Pilling, T.J. Wallington, The Mechanism of Atmospheric Oxidation of the Oxygenates, Oxford University Press, 2011, pp. 992–995.
- [36] J. Desai, J. Heicklen, A. Bahta, R. Simonaitis, The photo-oxidation of *i*- $\text{C}_3\text{H}_7\text{CHO}$  vapour, *J. Photochem.* 34 (1986) 137–164.